Journal of Micropalaeontology, **17**: 71–85. 0262-821X/98 $10.00

Late Miocene calcareous nannofossil genus *Catinaster*: taxonomy, evolution and magnetobiochronology

ALYSSA PELEO-ALAMPAY,[1] DAVID BUKRY,[2] LI LIU[3] & JEREMY R. YOUNG[4]

[1] Scripps Institution of Oceanography, University of California, San Diego, La Jolla, CA 92093–0208, USA; now at National Institute of Geological Sciences, University of the Philippines, Diliman, Quezon City, Philippines 110.
[2] U.S. Geological Survey, Paleontology and Stratigraphy Branch, 345 Middlefield Road, MS 915, Menlo Park, CA 94025, USA; now at Scripps Institution of Oceanography, University of California, San Diego, La Jolla, CA 92093–0231, USA.
[3] Department of Geology, Florida State University, Tallahassee, FL 32306, USA.
[4] Palaeontology Department, The Natural History Museum, London, SW7 5BD, UK.

ABSTRACT – A systematic study on the evolution and stratigraphic distribution of the species of *Catinaster* from several DSDP/ODP sites with magnetostratigraphic records is presented. The evolution of *Catinaster* from *Discoaster* is established by documentation of a transitional nannofossil species, *Discoaster transitus*. Two new subspecies, *Catinaster coalitus extensus* and *Catinaster calyculus rectus* are defined which appear to be intermediates in the evolution of *Catinaster coalitus coalitus* to *Catinaster calyculus calyculus*. The first occurrence of *C. coalitus* is shown to be in the lower part of C5n.2n at 10.7–10.9 Ma in the low to mid–latitude Atlantic and Pacific Oceans. The last occurrence of *C. coalitus coalitus* varies from the upper part of C5n.2n to the lower portion of C4A. Magnetobiostratigraphic evidence suggests that the FO of *C. calyculus rectus* is diachronous. *Catinaster mexicanus* occurs in the late Miocene and has been found only in the eastern equatorial Pacific, the Indian Ocean and the Gulf of Mexico. *J. Micropalaeontol.* **17**(1): 71–85, April 1998.

INTRODUCTION

The genus *Catinaster* and two of its species were first described by Martini & Bramlette (1963) from the 'middle' Miocene of Trinidad. The first occurrences of *Catinaster coalitus* and *Catinaster calyculus* are nannofossil zonal markers in the widely used zonations of Martini (1971) and Okada & Bukry (1980). As Berggren *et al.* (1995) noted, there are discrepancies of > 1 m.y. in published correlations of these and a few other early Tortonian markers making this interval one of the most unclear in the entire Tertiary for nannofossil–magnetostratigraphy integration. The stratigraphic distribution of *C. mexicanus* is known only from a few locations, and the relationship among these and other undescribed species of *Catinaster* have yet to be established. In this paper, we present data on the stratigraphic range, evolution and geographic distribution of catinasters from various Deep Sea Drilling Project (DSDP) and Ocean Drilling Program (ODP) sites from low to mid–latitudes (Fig. 1). We also describe a new subspecies, *Catinaster coalitus extensus* and document its stratigraphic distribution along with a transitional form between *Discoaster* and *Catinaster*. A new subspecies *C. calyculus rectus* is described which is older than *Catinaster calyculus calyculus*.

All species assigned to *Catinaster* are closely related to discoasters, hence to determine evolutionary relationships of this group a basic understanding of homology in Neogene discoasters is essential (Fig. 2m). These homologies have been dealt with in a number of papers (e.g. Stradner & Papp, 1961; Prins, 1971; Theodoridis, 1984; Perch–Nielsen, 1985). Typical

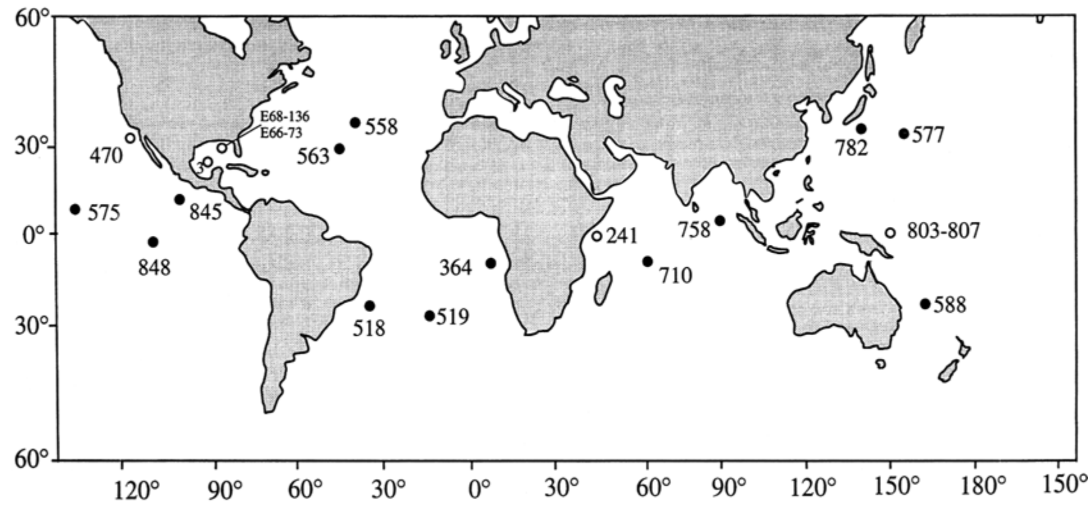

Fig. 1. Location map of DSDP/ODP sites investigated in this study. Closed circles indicate sites examined in the present study while open circles refer to sites cited in the text.

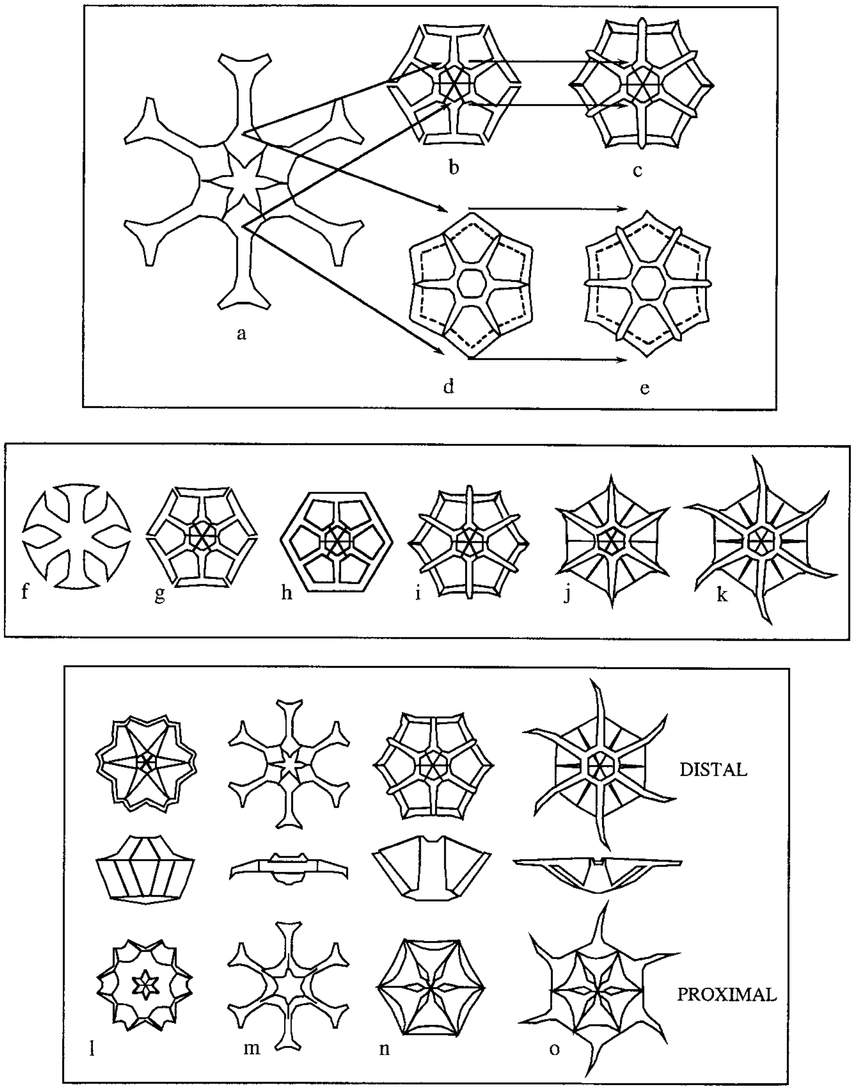

Fig. 2. *Catinaster* origins, development and morphology (modified from Young, unpublished PhD Thesis). **(a–e)** Origins. Distal views of *C. coalitus* (simple forms b, d; more complex, later forms c,e) and a *D. exilis* group discoaster. Sequence a–b–c: implied homologies of evolutionary sequence proposed by Martini & Worsley (1971). Sequence a–d–e: alternative homologies suggested by Theodoridis (1984). Morphological details such as the rim breaks and central area sutures shown in figs 2b and 2c suggest that sequence a–b–c is most likely. **(f–k)** Developmental Sequence: Distal views illustrating evolution from *Discoaster transitus* to *C. calyculus calyculus*. f: *D. transitus*; g: early *C. coalitus coalitus*; h: late *C. coalitus coalitus*; i: *C. coalitus extensus*; j: *C. calyculus rectus*; k: *C. calyculus calyculus*. **(l–o)** Comparative Morphology: Distal (top row), cross–section (centre row), and proximal (bottom row) views of: l, *C. mexicanus*; m, *D. exilis*; n, *C. coalitus coalitus*; o, *C. calyculus calyculus*.

Neogene discoasters (Fig. 2m) are star-shaped and formed of five or six rays often with bifurcate tips. Many species are concavo–convex which allows proximal (concave) and distal (convex) sides to be defined. In addition, central area structures can be used to consistently separate these two sides. On the distal side of the central area, low ridges usually run along the sutures, and if a stellate boss is developed, then it will show the same inter-radial orientation. Conversely, on the proximal side radially-directed stellate bosses and radial ridges are developed. These central area structures are developed to varying degrees in different species but their orientations are entirely consistent whenever they are present (Fig. 2m).

MATERIALS AND METHODS

Samples were taken from DSDP/ODP sites (Fig. 1) for which moderate to good magnetostratigraphies have been established for the chron 4–5 interval. These included Holes 519, 558, 563, 588/588A, 710A, 710B, 782A and 845A. A few sites without magnetostratigraphic records were also used to determine the occurrence and stratigraphic distribution of *C. mexicanus* and to study the evolution of catinasters. Relevant observations from a previous study of Indian Ocean DSDP Sites (Young, unpublished PhD Thesis) are also incorporated.

Smear slides were made from unprocessed marine sediment samples mounted with Norland optical adhesive and cured under ultraviolet light. Some mobile mounts in Canada balsam were made to photograph the same specimens in different orientations. Observations were done on a Zeiss Axioskop light microscope at 400× and 1000× magnification. All counts were done in phase contrast illumination.

Nannofossil abundances were estimated under 400× magnification using the following scheme modified from Gartner (1992):

A = abundant: 6–25 specimens per field of view.
C = common: 1–5 specimens per field of view.
F = few: 1 specimen in 2–10 fields of view.
R = rare: 1 specimen in 11–50 fields of view.
T = trace: 1 specimen in 51–200 fields of view.

Extra scanning time (45–60 min/slide) was spent to establish endpoint occurrences or null occurrences in the next few samples.

Magnetostratigraphies for Sites 519, 558, 563, 588, 710, 782 and 845 are from Poore *et al.* (1984), Kahn *et al.* (1985), Miller *et al.* (1985), Barton & Bloemendal (1986), Backman *et al.* (1990), Ali *et al.* (1992) and Mayer *et al.* (1992) and Schneider (1995), respectively. Detailed information about these sites such as core recovery, lithology, etc. can be found in DSDP/ODP Volumes 73, 82, 90, 115, 125 and 138. First and last occurrences of nannofossil species are assigned as the midpoint depth between productive and non-productive core samples. This midpoint depth is correlated to site magnetostratigraphy and later assigned an age, based on calibrations to the revised geomagnetic polarity time scale (GPTS) of Cande & Kent (1995). The quality of the magnetostratigraphy is assessed for each of the DSDP/ODP sites selected. For most of the sites, magnetostratigraphic interpretation is only broadly constrained by nannofossil biostratigraphy, thereby the problem of circularity in interpretation is minimal. Uncertainties in chron assignments and their bearing on the reliability of nannofossil datums are discussed in the text. It should be noted that in the calibration of datum depths to chron C5n.2n for sites with missing chrons C5n.1n and C5n.1r (Sites 519, 558, 563, 588 and 782), the duration of C5n.2n (9.920–10.949 Ma) is calculated from the top of C5n.1n to the bottom of C5n.2n (9.740–10.949 Ma). Chron terminology is from Cande & Kent (1992, 1995). Chron placements and age estimates of nannofossil datums from this study are compared with other DSDP/ODP nannofossil logs and with the revised Cenozoic biochronology of Berggren *et al.* (1995). Use of this biochronology places the entire *Catinaster* lineage in the late Miocene. All age estimates from previously published work are converted to the Cande & Kent (1995) GPTS.

Type specimen slides of new taxa presented here are deposited at the Scripps Institution of Oceanography Nannofossil Laboratory Collection with catalogue numbers recorded in the systematic descriptions.

RESULTS AND DISCUSSION

Abundance and range charts of *Catinaster* taxa from the different DSDP/ODP sites, arranged in chronological order are shown in Figs 3 and 4. The distribution patterns of *Catinaster coalitus coalitus*, *C. calyculus rectus* and *C. calyculus calyculus* from eight DSDP/ODP sites are summarized in Fig. 5. A section is devoted to these *Catinaster* taxa because they are more abundant in the sediments and have a more widespread occurrence than the other catinasters; this makes them good biostratigraphic markers for the Miocene. A separate section is presented for *Catinaster mexicanus* to synthesize data on this poorly documented species.

Evolutionary trends in *Catinaster*

Catinasters and their various transitional forms were documented from nine DSDP/ODP drillholes (519, 558, 563, 588, 710A, 710B, 758A, 782A and 845A). The following *Discoaster* and *Catinaster* taxa were recognized (Fig. 2 f–k):

Discoaster transitus
Catinaster coalitus coalitus
Catinaster coalitus extensus
Catinaster calyculus rectus
Catinaster calyculus calyculus
Catinaster mexicanus.

Because of the susceptibility of catinasters to overgrowth, all six forms were rarely recognized in a single site. A probable evolutionary scheme for genus *Catinaster* is shown in Fig. 6. These species and subspecies are described in detail in the sytematics section.

Evolution of the genus *Catinaster* from *Discoaster* has previously been suggested based on morphology i.e. similarity of the two genera, and partly on stratigraphic occurrence. Martini & Worsley (1971) proposed that *C. coalitus* evolved from 'a small discoaster resembling *D. extensus* by becoming highly concavo–convex and reducing the interray areas until they are closed' (Fig. 2 a–c). Bukry (1973) suggested a possible derivation of *C. coalitus* from *Discoaster bollii* by reduction of the rays while Martini (1981) proposed that *D. musicus* gave rise to *Catinaster*. An alternative view was given by Theodoridis (1984) who defined *C. coalitus* (*Eu-discoaster coalitus* group) as 'asteroliths with ... pronounced sutural ridges on the distal face of the central area' and stated that they lack arms (Fig. 2 a,d,e). This implies a different evolutionary scheme from that proposed by the previous nannofossil workers. Structures considered as rays by Martini & Worsley (1971) and Bukry (1973) are sutural ridges to Theodoridis (1984). The interpretation favouring rays instead of sutural ridges is supported by the following observations: (a) the presence of *C. coalitus* specimens with slight breaks in the rim on the distal side that suggest incomplete fusion of the bifurcated rays (Fig. 2g; Pl. 1, fig. 1; Pl. 2, figs 12–13); a feature that would not be compatible with Theodoridis' sutural ridges ; (b) a proximal view of a well-preserved specimen in Müller (1974; pl. 10, fig. 4) shows a stellate central structure which is oriented parallel to the ridges on the opposite face suggesting that the ridges on the distal face are rays; (c) ridges extend as free rays in *C. calyculus*; and (d) the presence of sutures between rays in the centre of *C. coalitus* (pl. 1, figs 1–3, 10; pl. 3, fig. 1 in Martini, 1981).

Thus, we interpret the basic morphology of catinasters as consisting of a cup formed by fusion of the bifurcations. This cup is open distally and closed proximally. The rays are arranged inside the cup as six radial plates, rather like the septa of a coral. They protrude distally above the cup, where they are surmounted by a concave disk derived from the reduced central

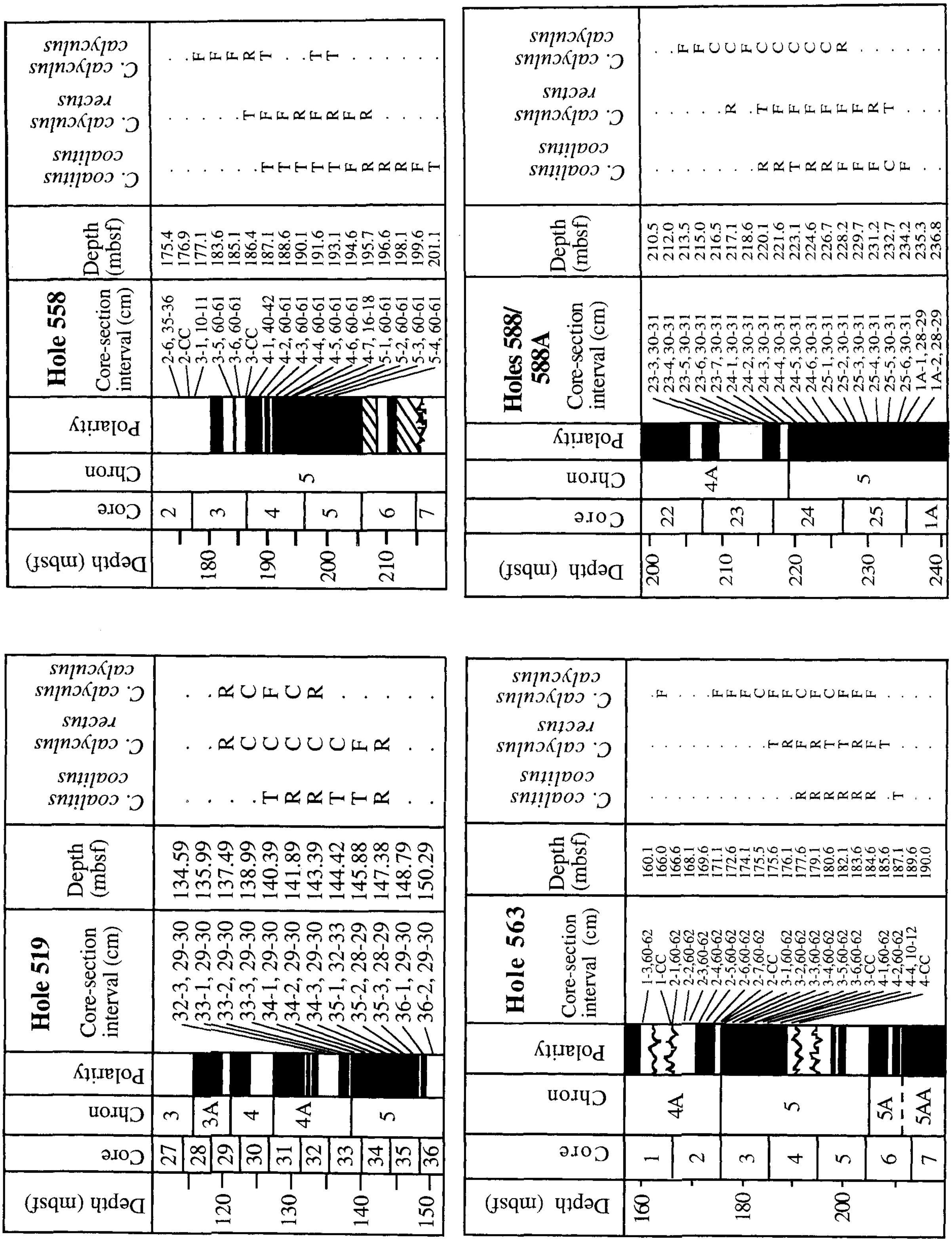

Fig. 3. Abundance patterns of *Discoaster transitus*, *Catinaster coalitus coalitus*, *Catinaster coalitus extensus*, *C. calyculus rectus* and *C. calyculus calyculus* in DSDP Sites 519, 558, 563 and 588 calibrated to site magnetostratigraphies. Sources for magnetostratigraphy: DSDP Hole 519, Poore *et al.* (1984); DSDP Hole 558, Kahn *et al.* (1985); DSDP Hole 563: Miller *et al.* (1985); DSDP Holes 588/588A, Barton & Bloemendal (1986). A = abundant; C = common; F = few; R = rare; T = trace; CC = core-catcher sample.

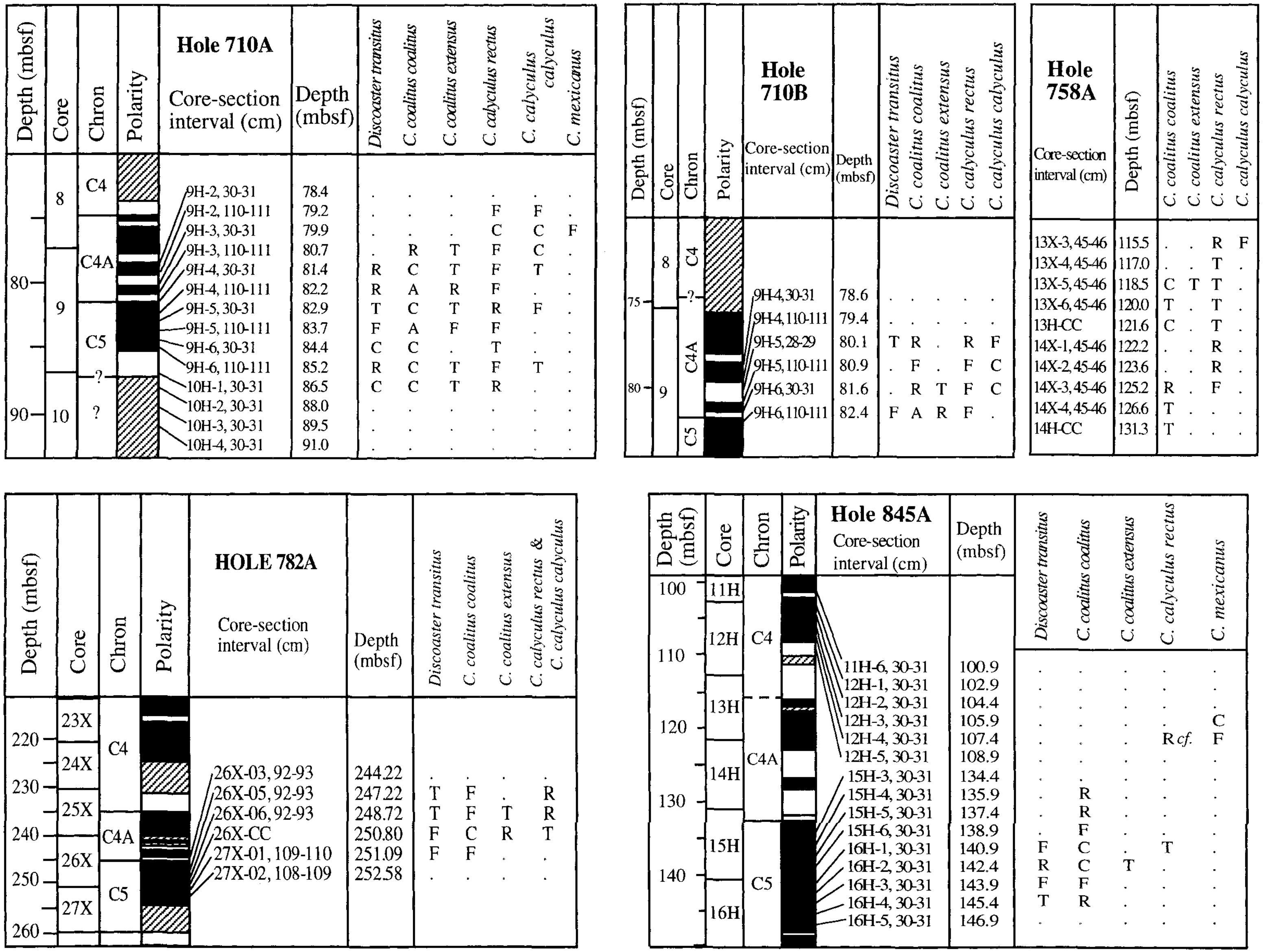

Fig. 4. Abundance patterns of *Discoaster transitus*, *Catinaster coalitus coalitus*, *Catinaster coalitus extensus*, *C. calyculus rectus* and *C. calyculus calyculus* in ODP Sites 710, 758, 782 and 845 calibrated to site magnetostratigraphies. Depth data for Hole 758A are from Peirce *et al.* (1989). Sources for magnetostratigraphy: ODP Holes 710A/710B, Backman *et al.* (1990) and Schneider & Kent (1990); ODP Hole 782A, Ali *et al.* (1992); and ODP Hole 845A, Mayer *et al.* (1992) and Schneider (1995). A = abundant; C = common; F = few; R = rare; T = trace; CC = core-catcher sample.

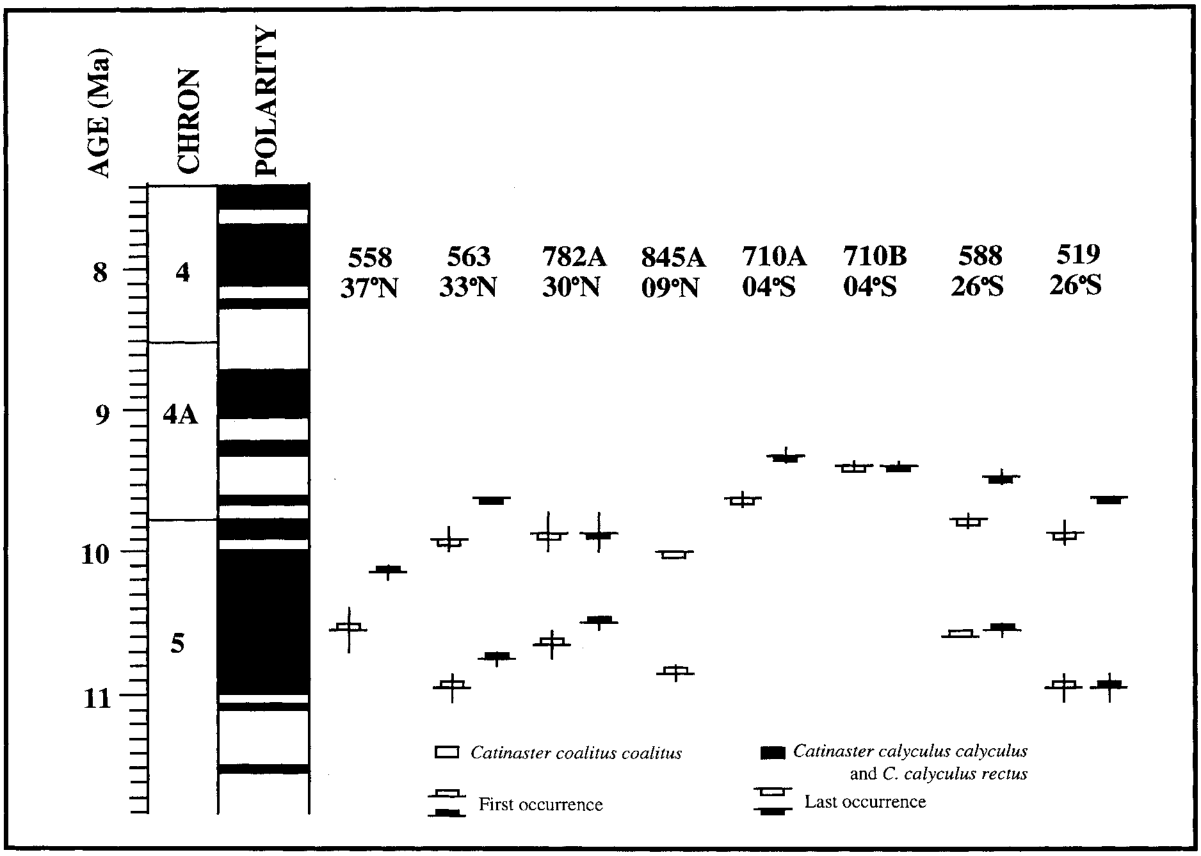

Fig. 5. Comparison of stratigraphic ranges of *Catinaster coalitus coalitus*, *C. calyculus calyculus* and *C. calyculus rectus* from DSDP/ODP sites with magnetostratigraphic records calibrated to the geomagnetic polarity time scale of Cande and Kent (1995). Sites are arranged from north to south according to latitude. In some sites, only FO and LO can be shown either due to a gap in the magnetostratigraphic record or absence of samples. Vertical bars represent the time interval between productive and non-productive samples. Horizontal bars represent the midpoint of this time interval at which the datum age is designated. Calibrations for both shorter and longer C5n.2n interpretations for Site 558 are included within the uncertainty values.

area. The proximal view is often complex showing both the base of the rays and the convergent bifurcations. Rays and bifurcations are usually readily identifiable in proximal view due to the presence of openings between the rays (Pl. 1, figs 5–6, 9, 13–14). They are less obvious in specimens without such openings (e.g. Pl. 1, fig. 15; Pl. 2, fig. 1).

In light microscopy, a key feature of *Catinaster* is that the rays extend through from the top to the base of the specimen, hence as one focuses through the specimen the orientation of the rays does not change. Discoasters such as *D. musicus* with massive central areas can produce specimens which look very similar to catinasters if they lose their rays, but they have a sutural star on the distal side with inverse orientation. Aubry (1993a) illustrated specimens of this type as *Catinaster* sp. (Pl. 3, figs 13–15, 17–19), and they strongly resemble specimens of *D. musicus* and *D. sanmiguelensis* from the same sample (Pl. 3, figs 5–7, 9–10).

The earliest forms we recognize are small discoasters with unusually thick cross–sections, converging on the cup–shaped morphology of *Catinaster*. These specimens have small central areas and strongly bifurcate rays but the tips of the bifurcations do not meet. We term these forms *Discoaster transitus* (Pl. 2, figs 9–11). Another small discoaster species has been described from sediments of this age – *Discoaster micros* (Theodoridis, 1984) de Kaenel & Villa 1996. *D. micros* like *D. transitus* has six rays with bifurcate tips. However, *D. micros* has a large central area and stubby bifurcations, in contrast to the small central area and large bifurcations of *D. transitus*. The *D. micros* morphology is inappropriate for evolution into *Catinaster coalitus* (cf. Fig. 2a–c, discussion above). We would not include the seven-rayed late Miocene form illustrated by de Kaenel and Villa (1996) in our concept of *D. micros*.

From this discoaster relative, early forms of *Catinaster coalitus coalitus* (Pl. 1, figs 1–3) evolved which have a significantly thicker cup-shaped morphology and smaller gaps between bifurcations. In later *C. coalitus coalitus* forms, the bifurcations fuse to form a continuous hexagonal rim (Pl. 1, fig. 4; Pl. 2, figs 14–15). Another subspecies, *Catinaster coalitus extensus*, succeeded *C. coalitus coalitus*, preserving the overall morphology of the latter but with all the rays extending out of the rim (Pl. 1, fig. 8; Pl. 2, figs 19–20; Pl. 3, figs 1–6). This subspecies is considered to be a transitional morphotype to *C. calyculus*. Abundance of *C. coalitus extensus* is quite low and it is

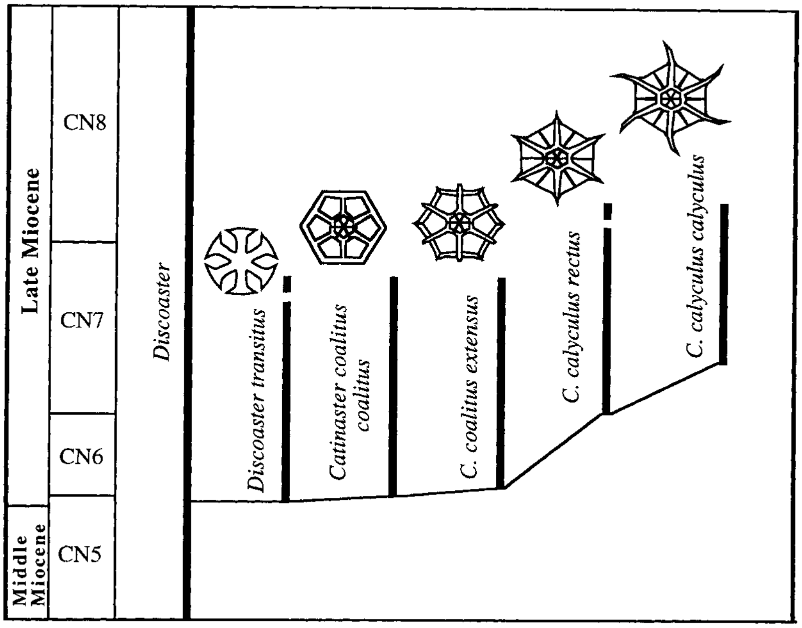

Fig. 6. Evolution of the *Catinaster* species from *Discoaster transitus*.

present only in relatively well preserved specimens. Its stratigraphic range is mostly limited to the middle–upper part of magnetic chron C5n.2n although it extends to chron C5r.1 and C4Ar.2n in Site 710.

Catinaster calyculus rectus subsequently evolved from *C. coalitus extensus* with six straight rays forming the corners of the hexagonal basket (Pl. 1, figs 10–14; Pl. 3, figs 7–8). In *C. calyculus*, the shape of the distal cup has changed as a result of the extruded rays. The simple hexagonal cup in *C. coalitus* whose corners are formed by fusion of adjoining bifurcating rays, has retracted towards the proximal pole in *C. calyculus*. Instead, the distal rim in *C. calyculus* is a modified hexagon with protruding corners formed by the extended rays and the retracted cup edges (compare Pl. 1, figs 1–4 with figs 10–12). Evidence from Holes 519, 558, 563, 588, 710A, 710B and 758A shows the later development of curved rays in *C. calyculus calyculus* (Pl. 1, figs 16–20; Pl. 3, figs 14–15) as suggested by Martini & Bramlette (1963) and Martini (1981). Ray curvature is consistently counter-clockwise in distal view (Pl. 1, figs 18–20). A new subspecies is erected to distinguish the form with straight rays, *C. calyculus rectus*, from the one with curved rays, *C. calyculus calyculus*. The first occurrence (FO) of *Catinaster calyculus calyculus* from different sites remains within subchron C5n.2. The last occurrence (LO) of *C. calyculus rectus* usually occurs at the same level as *C. calyculus calyculus* but in three sites (558, 563 and 588), it disappeared earlier.

Because of its very limited occurrence, it is difficult to ascertain whether *Catinaster mexicanus* (Pl. 2, figs 2–8; Pl. 3, figs 17–20) evolved from the rest of the catinasters. We know that it evolved later than the rest of the *Catinaster* species based on reported occurrences and its association with CN7–CN9a nannofossils. Young (unpublished) suspects that *C. mexicanus* is an unrelated homoeomorph of the catinasters that evolved by ray reduction (evolutionary sequence a–d–e of Fig. 2) because of the presence of 'sutural ridges on the distal side', a feature absent in typical catinasters. Alternatively, Young (unpublished) believes that *C. mexicanus* could be a 'preservational fragment of a discoaster rather than a genuine species' and Pujos (1985) considered it as a relict of *D. tristellifer* (syn. *D. altus*).

Our SEM illustrations (especially Pl. 2, fig. 2) clearly show sutures running through the ridges on the distal side. Thus these ridges cannot be homologous with the ridges in the distal side of *C. coalitus* or *C. calyculus*. This suggests an independent origin of *C. mexicanus* from discoasters. On the other hand, *C. mexicanus* has the hexaradiate symmetry and cup shape that is characteristic of the catinasters. *C. mexicanus* could be a second derivation from *Discoaster*, separate from the two other species or it could have been the result of mutation at the end of the *Catinaster* line. A more specific possible explanation is that it evolved from *C. coalitus* by infilling of the spaces between the rays followed by expansion of the central area and development of new sutural ridges. Affinity with the catinasters is also suggested by the stratigraphic co-occurrence of *C. mexicanus* and *C. calyculus rectus* in three sites (Sites 3, 710A and 845A). Lacking any other evidence for definitive relatives of this species, we tentatively continue to include it with the catinasters, but exclude it from our evolutionary scheme.

FO and LO of *Catinaster coalitus coalitus*, *C. calyculus calyculus* and *C. calyculus rectus*

C. coalitus coalitus, *C. calyculus calyculus* and *C. calyculus rectus* were identified based on a modified species concept which enabled us to make consistent determinations of the three taxa (Peleo-Alampay & Wei, 1995). Previously, the main distinction between *C. coalitus* and *C. calyculus* is the extension of the rays beyond the rim in the latter. We define the species concept of *C.*

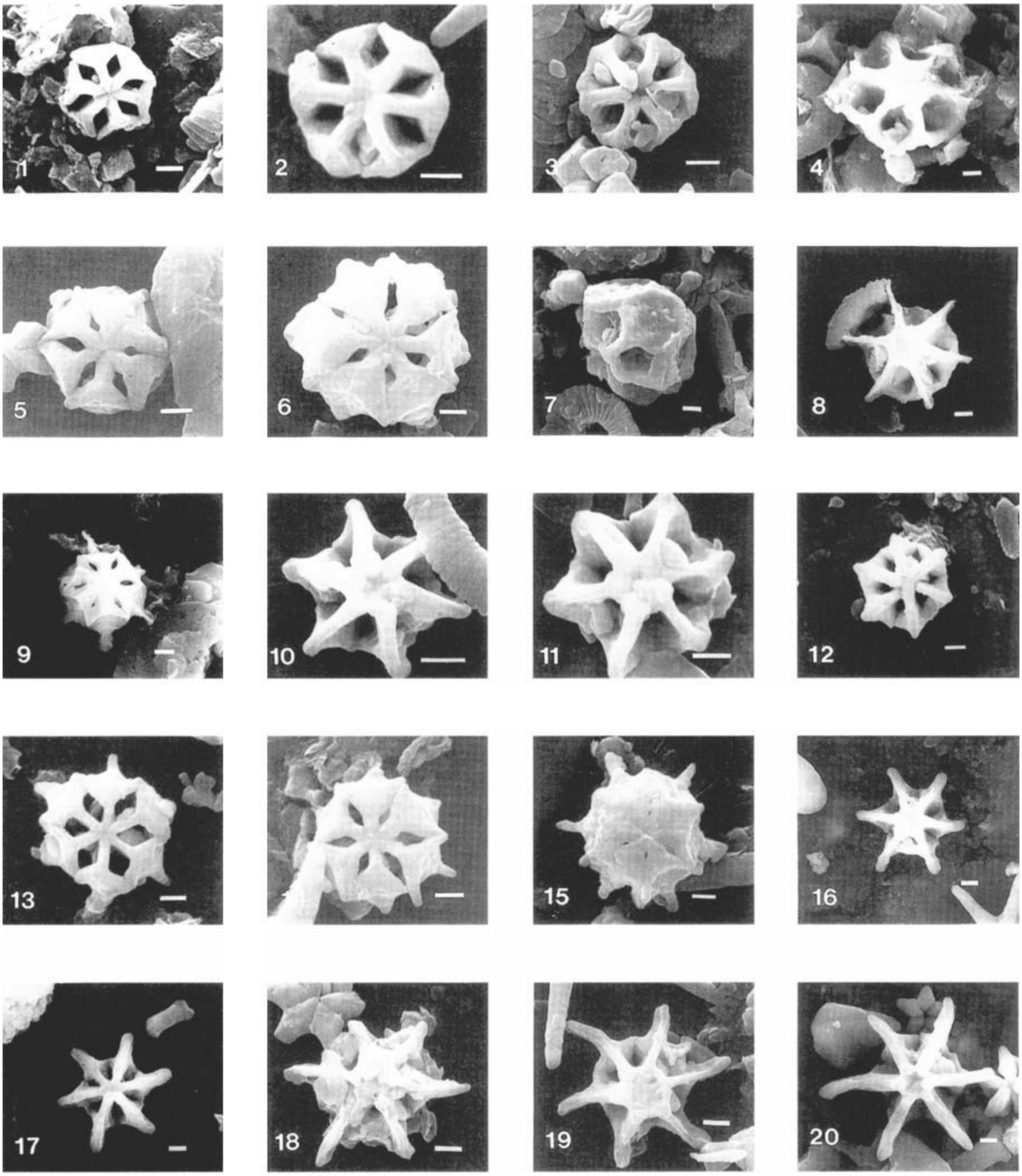

Explanation of Plate 1

All figures are SEM micrographs. White bar = 1 μm.
Fig. 1: ODP Sample 710A-9H-4, 110-111 cm. **figs 2–3, 5–7, 12–15:** ODP Sample 710A-9H-5, 110–11 cm. **figs 4, 8–9, 16–17, 20:** ODP Sample 782A-26X-CC. **figs 10–11, 18–19:** ODP Sample 710A-9H-3, 30–1 cm.
figs 1–4. *Catinaster coalitus coalitus*, distal view. figs 5–6. *Catinaster coalitus coalitus*, proximal view. fig. 7. *Catinaster coalitus coalitus*, side view; distal surface toward top right. fig. 8. *Catinaster coalitus extensus*, distal view. fig. 9. *Catinaster coalitus extensus*, proximal view. figs 10–12. *Catinaster calyculus rectus*, distal view. figs 13–15. *Catinaster calyculus rectus*, proximal view. figs 16–20. *Catinaster calyculus calyculus*, distal view.

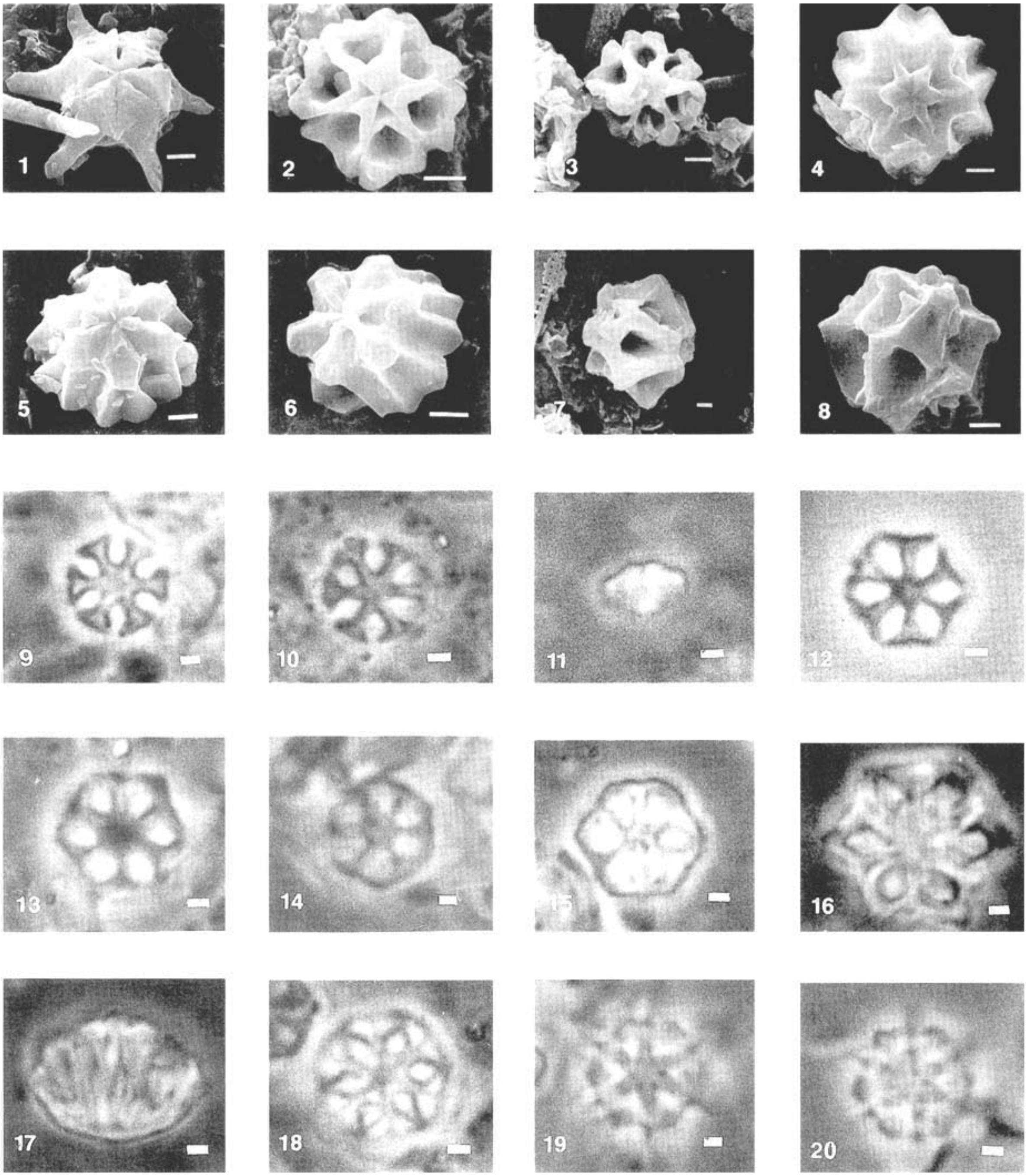

Explanation of Plate 2

Figs 1–8 are SEM micrographs. **figs 9–20** are phase contrast light micrographs. White bar = 1 μm.
Fig. 1: ODP Sample 710A-9H-3, 30–31 cm. **figs 2, 4–6, 8:** ODP Sample 845A-12H-3, 30–31 cm. **figs 3, 7:** ODP Sample 845A-12H-4, 30–31 cm. **figs 9–11, 13, 15, 18:** ODP Sample 710A-10H-1, 30–31 cm. **fig. 12:** ODP Sample 845A-16H-1, 30–31 cm. **figs 14, 20:** ODP Sample 710A-9H-4, 110–111 cm. **figs 16–17:** ODP Sample 782A-26X-CC. **fig. 19:** ODP Sample 710A-9H-5, 110–111 cm.
fig. 1. *Catinaster calyculus calyculus*, proximal view. figs 2–3. *Catinaster mexicanus*, distal view. figs 4–6. *Catinaster mexicanus*, proximal view. figs 7–8. *Catinaster mexicanus*, side view. figs 9–10. *Discoaster transitus*, distal view. fig. 11. *Discoaster transitus*, side. figs 12–15. *Catinaster coalitus coalitus*, distal view. figs 16–17. *Catinaster coalitus coalitus*, mobile mount; Fig. 16, proximal; Fig. 17, side. fig. 18. *Catinaster coalitus coalitus*, proximal view. figs 19–20. *Catinaster coalitus extensus*, distal view.

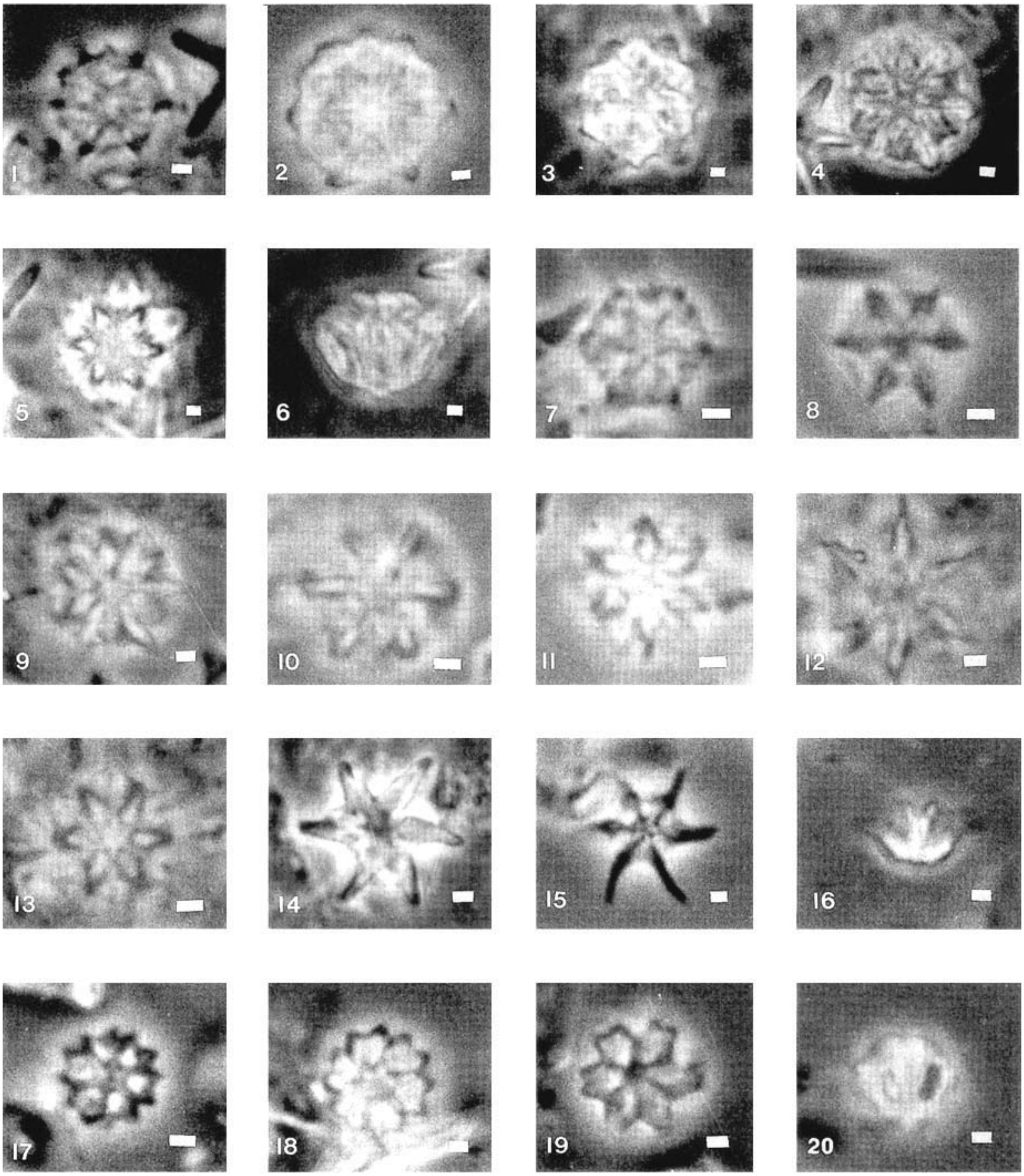

Explanation of Plate 3

All figures are phase contrast light micrographs. White bar = 1 μm. **fig. 1:** ODP Sample 710A-9H-5, 30–31 cm. **figs 2–6, 9:** ODP Sample 710A-9H-5, 110–111 cm. **fig. 7:** ODP Sample 710A-9H-4, 110–111 cm. **figs 8, 14–16:** ODP Sample 710A-9H-3, 30–31 cm. **figs. 10–13:** ODP Sample 710A-9H-4, 30–31 cm. **figs. 17–20:** ODP Sample 845A-12H-4, 30–31 cm.

figs 1–2. *Catinaster coalitus extensus*, distal view. Note the pseudorays in the rim of fig. 2. figs 3–6. *Catinaster coalitus extensus*, mobile mount; fig. 3, distal; fig. 4, proximal, low focus; fig. 5, proximal, high focus; fig. 6, side. figs 7–8. *Catinaster calyculus rectus*, distal view. fig. 9. *Catinaster calyculus rectus*, proximal view. figs 10–11. *Catinaster calyculus rectus*, same specimen. fig. 10, low focus, distal; fig. 11, high focus, proximal. figs 12–13. *Catinaster calyculus calyculus*, same specimen. fig. 12, low focus, distal; fig. 13, high focus, proximal. fig. 14. *Catinaster calyculus calyculus*, proximal view. fig. 15. *Catinaster calyculus calyculus*, distal view. fig. 16. *Catinaster calyculus calyculus*, side view. figs 17–18. *Catinaster mexicanus*, distal view. fig. 19. *Catinaster mexicanus*, proximal view. fig. 20. *Catinaster mexicanus*, side view.

coalitus coalitus as catinasters whose rays connect to the middle of the segments of the basket rather than the corners when observed under the light microscope. On the other hand, the rays of *C. calyculus calyculus* and *C. calyculus rectus* extend to form corners of the rim (see systematic descriptions). This distinction between the two species is due to modifications in the shape of the distal rim as a result of ray extension in *C. calyculus* (refer to discussion in evolution). This definition is especially helpful in classifying transitional morphotypes (e.g. *C. coalitus* with rays extending out of the rim) whose identification was based on the old distinction between the two species (i.e. whether the rays extend out of the basket).

Berggren *et al.* (1995) provide two alternative placements for the FO of *C. coalitus*, either at 10.9 Ma (Chron C5n.2n) based on data from equatorial Pacific sites or at 11.3 Ma (subcron C5r.2r), based on Atlantic sites. From our examination of several Miocene Atlantic and Pacific sites with magnetostratigraphies, the FO of *C. coalitus coalitus* is consistently in the lower part of subchron C5n.2n (10.55–10.95 Ma). This result coincides with the report of Berggren *et al.* (1995) from the equatorial Pacific (10.9 Ma; based on Raffi & Flores, 1995 and Raffi *et al.*, 1995) but is significantly different from the placement of this datum in subchron C5r.2r (11.3 Ma). One of their bases for this latter datum report is Miller *et al.* (1985) who recorded *C. coalitus coalitus* down through the bottom of core 4 in Hole 563. As in Parker *et al.* (1985), we did not find any *C. coalitus coalitus* in the lower part of core 4 despite extensive search. Berggren *et al.* (1995) also cited Site 710 (Raffi *et al.*, 1995) as another reference for placement of this datum in C5r.2r, as was reported by Miller *et al.* (1994) in the Buff Bay Section of Jamaica. Our observations of the FO of *C. coalitus coalitus* at Hole 710A is consistent with that of Raffi *et al.* (1995) but a proper chron calibration is not possible because this core (710A–10H) has evidence of slumping, hence no magnetic chron was designated in the ODP reports. Our results from other sites are consistent with previous reports from Hole 782A (Xu & Wise, 1992), Site 588 (Lohman, 1986), Hole 845A (Raffi *et al.*, 1995) and Site 519 (Poore *et al.*, 1984). An equivalent age was adopted by Young *et al.* (1994). The rarity and presence of overgrowth on *C. coalitus coalitus* specimens in some sites can pose a problem in establishing a consistent age estimate for this datum. Identification of the long normal Chron 5n.2n where the FO of *C. coalitus coalitus* occurs is straightforward for most of the sites. The lower boundary of C5n.2n in Site 558 may be reinterpreted to include the next indeterminate interval which extends the bottom depth of this subchron to 208 mbsf. This results in a younger estimated age for the FO datum (Fig. 5). Although discontinuities in the magnetostratigraphic record of Hole 782A exist, a datum calibration consistent with other sites was found.

In most of the sites, the LO of *C. coalitus coalitus* corresponds to the upper part of C5n.2n (9.75–10.0 Ma) but in ODP Holes 710A and 710B and DSDP Hole 558, it corresponds to C4A. In these three cores, the magnetostratigraphy can be subject to reinterpretation especially at this interval (C4A–C5) because of the slumped reworked sediments above and below core 710A–9H, no recovery above and below core 710B–9H, and an incomplete record at Site 558. A reliable age estimate for this datum cannot be made at Site 558 due to difficulty in interpreting specific subchrons above C5n.2n. Our results closely agree with previous work from Site 519 (Poore *et al.*, 1984), Site 558 (Parker *et al.*, 1985), Site 563 (Miller *et al.*, 1985; Parker *et al.*, 1985; Peleo–Alampay & Wei, 1995), Site 710 (Rio *et al.*, 1990; Backman *et al.*, 1990) and Hole 782A (Xu & Wise, 1992). The discrepancy between our LO datum depth (219.35 mbsf) in Site 588 and that of Lohman (1986) at 213.96 mbsf may be attributed to differences in species concepts of *C. calyculus rectus* and *C. coalitus coalitus* although we did not find *C. calyculus rectus* up to that depth (refer to Hole 588/588A abundance chart).

The FO of *C. calyculus rectus* is in the lower portion of C5n.2n (10.75–10.95 Ma) in Sites 519 and 563, and coincides with the FO of *C. coalitus coalitus* in Site 519. In other sites (558, 588 and 782) however, *C. calyculus rectus* appeared later in mid–upper C5n.2n. At Holes 558, 563, 588 and 782A, we found this datum lower than previously reported, resulting in a 0–0.3 m.y. variation in age. Our datum depth of 186.35 mbsf at Site 563 is close to 185.1 mbsf as reported by Parker *et al.* (1985), Miller *et al.* (1985) and Peleo-Alampay & Wei (1995) from the same site, giving a consistent age estimate of 10.75 Ma. In Site 558, Parker *et al.* (1985) recorded this FO datum at 193.85 mbsf while we report it at 196.13 mbsf. Age estimates from this site do not change significantly when the lower boundary of C5n.2n is extended to the bottom of the indeterminate interval. We placed this datum at 233.45 mbsf (10.55 Ma) in Site 588, compared to Lohman's (1986) datum depth at 230.16 mbsf (10.35 Ma). At Hole 782A, we located it at 250.54 mbsf as opposed to 248.72 mbsf (Xu & Wise, 1992). In Site 519 however, we got a significantly deeper depth (148.1 mbsf; 10.95 Ma) for this datum than Percival (1984) and Poore *et al.* (1984) who reported it at 141.55 mbsf (10.1 Ma). This discrepancy can be due to a difference in species concepts of *C. coalitus coalitus* and C. *calyculus rectus* (refer to Hole 519 abundance chart). We were not able to establish reliable FO and LO datums for *C. calyculus* subspecies at Hole 845A where they had a very limited occurrence although Raffi *et al.* (1995) were able to determine a FO datum for *C. calyculus* by analysing samples from both Hole 845A and 845B. Raffi *et al.* (1995) reported the FO datum depth at 158.72 mcd (10.45 Ma). The discrepant age estimates for this datum signify possible diachroneity of the FO of *C. calyculus rectus* as suggested in Peleo-Alampay & Wei (1995). The coincidence of the FO of *C. coalitus coalitus* and *C. calyculus rectus* (with straight rays) at Site 519 might seem to contradict the nannofossil zonation of Okada & Bukry (1980) which utilizes the FO of *C. coalitus coalitus* and *C. calyculus calyculus* (with curved rays) to delineate the base of Zone CN6 and Subzone CN7b, respectively. Similarly, this apparent coincidence violates the evolutionary sequence presented in our Fig. 6, and therefore, reflects the missing section at Site 519 or incomplete sampling of the local ranges.

Most detailed studies, including this one, support the sequence of *C. coalitus coalitus* preceding *C. calyculus calyculus*. For example, Takayama (1993) detailed species events from five ODP drillholes (803D, 804C, 805B, 806B and 807A) on the Ontong–Java Plateau in the tropical Pacific and showed that the FO of *C. coalitus coalitus* is consistently found earlier than the FO of *C. calyculus calyculus*. These consistent results support the utility of catinaster occurrences for identifying Zone CN6 and Subzone CN7b of Okada & Bukry (1980) for low latitude floras.

The LO of *C. calyculus calyculus* is in the lower part of C4A (9.3–9.6 Ma). Results from our analysis of this datum are exactly consistent with previous reports from Site 563 (Parker *et al.*, 1985; Peleo-Alampay & Wei, 1995), Hole 782A (Xu & Wise, 1992) and Site 519 (Poore *et al.*, 1984). Our calibration of this datum at Site 588 is at a shallower depth (212.73 mbsf) than the 213.96 mbsf observed by Lohman (1986), corresponding to a 0.1 m.y. difference in age estimates. The older age estimate of 9.85 Ma from Hole 782A could be due to poor preservation in that site as compared to others.

Catinaster mexicanus

Catinaster mexicanus was described by Bukry (1971) from DSDP Site 3 in the Gulf of Mexico where it was given an upper Miocene age. It has only been recorded in a few sites since. Ellis *et al.* (1972) also recorded *C. mexicanus*, along with *C. coalitus*, in Site 3. Aside from DSDP Site 3, *C. mexicanus* has been reported from the Somali Basin in the western Indian Ocean (DSDP Leg 25) by Müller (1974) where it was assigned an upper Pliocene age (NN15) although specimens were considered atypical. The bifurcation of the rays seemed less distinct than those described from the Miocene. In Leg 85, Pujos (1985) noted the similarity of *C. mexicanus* specimens in mid–Pliocene zones CN11 and CN12a to the knobbed centre of *D. tristellifer* and classified it under the latter. Bukry (1981) documented *C. mexicanus* from the west coast of Mexico and found it associated with Zone CN8 and CN9 coccoliths in the late Miocene. Jiang & Watkins (1992) documented the occurrence of *C. mexicanus* in nannofossil subzone CN9a (late Miocene) from the northern Gulf of Mexico. In the same region, Aubry (1993a) reported the presence of *C. coalitus coalitus* with *C. mexicanus* in two Eureka drill sites (Coreholes E68–136 and E66–73). In both drill sites, this co-occurrence cannot be firmly established due to reworking and mixing in the older sediments (Zones CN4–CN6). The same is true for the younger intervals (Subzones CN7a and CN9a) where poor preservation and low abundance hampered definite identification of *C. coalitus coalitus* (particularly in Corehole E68–136). It is also possible that the *C. coalitus* specimens identified (especially in the critical sample 2433'9", Hole E68–136 where they are most abundant) are *D. musicus*/*D. sanmiguelensis* with reduced rays. Aubry (1993*a*) however, recognized *C. mexicanus* without *C. coalitus coalitus* in one sample in Subzone CN9a.

We found *C. mexicanus* in Hole 845A in the eastern equatorial Pacific Ocean, Hole 710A in the Indian Ocean and Site 3 in the Gulf of Mexico. We did not find it in the Miocene sediments we examined from Holes 364, 518A, 519, 563, 575A, 577A, 588, 588A, 710B, 758A and 848B. At Hole 845A, it co-occurs with *Catinaster calyculus rectus cf.* in Subzone CN9a where the nannofossil assemblage primarily consists of *Discoaster quinqueramus, D. brouweri, D. challengeri, D. variabilis, D. berggrenii, D. surculus* and *D. pentaradiatus* with the noticeable absence of *Amaurolithus*. This is similar to the report of Bukry & Bramlette (1969) from Site 3. *C. calyculus rectus* specimens observed (by A. P.-A.) in Hole 845A are similar to those observed in Site 3 co-occurring with *C. mexicanus* where the rays do not extend beyond the rim. Most of their rims are dissolved and the ray tips show some overgrowth. At Hole 710A however, *C. mexicanus* is associated with *D. hamatus* in Zone CN7. Locations of reported occurrences of *C. mexicanus* suggests a preference for particular environments such as semi-enclosed basins or in locations proximal to the continental borderland (Sites 241, 470A and 845A). Correlation with site water depths has not been found.

CONCLUSIONS

The evolution of *Catinaster* from *Discoaster* and among the *Catinaster* species is established with the documentation of a transitional form, *Discoaster transitus* and a new subspecies, *Catinaster coalitus extensus*. New subspecies, *Catinaster calyculus rectus* gave rise to *C. calyculus calyculus* which is used to identify Subzone CN7b.

The FO of *C. coalitus coalitus* is shown to be consistently at the lower part of C5n.2n at 10.55–10.95 Ma. The LO of *C. coalitus coalitus* is at the upper part of C5n.2n (9.75–10.0 Ma) in most sites but extends up to the lower portion of C4A (9.4–9.6 Ma) in some sites. The FO of *C. calyculus rectus* appears earlier at the lower part of C5n.2n in some sites, even coinciding with the FO of *C. coalitus coalitus*, while it occurs later in others (mid–upper C5n.2n). This suggests diachroneity of this subspecies. Similarly, *C. calyculus calyculus* appears in lower to mid-C5n.2n at five of our sections and higher at two others.

Catinaster mexicanus has a very limited geographic distribution and seems to prefer specific environments. It usually occurs in the late Miocene within nannofossil zones CN7–CN9a.

SYSTEMATIC DESCRIPTIONS

Family **Discoasteraceae** Tan, 1927

Genus *Discoaster* Tan, 1927

Discoaster transitus **n. sp.**

(Pl. 2, figs 9–11)

Derivation of name. Latin, *transitus*, transition; referring to this species being transitional in morphology and evolution between *Catinaster* and *Discoaster*.

Holotype. Pl. 2, fig. 9; SIO–NLC # 018–001.

Type Locality. Ocean Drilling Program Hole 710A in the central Madingley Rise, western equatorial Indian Ocean (04° 18.7'S, 60° 58.8'E); ODP Sample 710A-10H-1, 30–31 cm.

Diagnosis. *Discoaster transitus* is a transitional species between *Discoaster* and *Catinaster*. It is a simple six–rayed discoaster with bifurcating ray ends. The sides of the rays are parallel until they reach the point of bifurcation. It has a small central area with no distinctive knob or suture pattern. In side view it is thicker than regular discoasters, a feature that is typical of *C. coalitus coalitus*. The bifurcated ray ends are not fused to form the outer rim as in typical catinasters. These transitional forms are generally smaller than typical discoasters.

Size. 3–6 μm.

Remarks. It is differentiated from *D. micros* by the presence of a reduced central area resulting in longer free rays, the long bifurcations, the lack of notched ray ends and a consistent six–rayed symmetry. Its small size distinguishes it from the larger *D. extensus* and *D. divaricatus* aside from being more robust–looking and lacking the distinct notch present in *D. divaricatus*.

Occurrence. Usually within the range of *C. coalitus coalitus* (within Chron C5) but disappears slightly earlier than *C. coalitus coalitus*.

Genus *Catinaster* Martini & Bramlette, 1963
Catinaster coalitus Martini & Bramlette, 1963

1963 *Catinaster coalitus* Martini & Bramlette: 851, pl. 103, figs 7–9
1967 *Catinaster coalitus* Martini & Bramlette; Bramlette & Wilcoxon: 108, pl. 8, figs 9–10
1971 *Catinaster coalitus* Martini & Bramlette; Martini: 784, pl. 4, fig. 4
1972 *Catinaster coalitus* Martini & Bramlette; Ellis *et al.*: 84, pl. 9, figs 5–6
1974 *Catinaster coalitus* Martini & Bramlette; Müller: 614–615, pl. 10, figs 1 and 3–5
1981 *Catinaster coalitus* Martini & Bramlette; Martini: 563, pl. 3, figs 1–4
1990 Non–*Catinaster coalitus* Martini & Bramlette; Rio *et al.*: 227, pl. 6, figs 11A–11B
1992 *Catinaster coalitus* Martini & Bramlette; Jiang & Watkins; 617, pl. 3, fig. 29
1992 *Catinaster coalitus* Martini & Bramlette; Xu & Wise: 70, pl. 5, figs 9–10, 17
1993*b* *Catinaster* sp.; Aubry: 171, pl. 16, figs 4–6
1993*b* *Catinaster calyculus* Martini & Bramlette; Aubry: 171, pl. 16, figs 11–14
1995 *Catinaster coalitus* Martini & Bramlette; Peleo-Alampay & Wei: 108, pl. 2, figs 1–3
1995 Non–*Catinaster coalitus* Martini & Bramlette; Peleo-Alampay & Wei: 108, pl. 2, fig. 4

Remarks. *C. coalitus* typically has six rays and a circular or hexagonal rim (Pl. 1, figs 1–4). This rim/basket is formed by the bifurcation of the rays. The hexagonal rim in *C. coalitus* has corners formed by the fused bifurcations. In the light microscope, this can be seen as rays that connect to the middle of the segments of the rim rather than the corners as in *C. calyculus* (Peleo-Alampay & Wei, 1995). The rim continues to the proximal side of the catinaster producing the basket-like body. In earlier forms, the bifurcated rays can have gaps between them, producing an incomplete rim (Fig. 2). In large *C. coalitus* specimens, pseudo-rays or nodes can be formed along the rim where the bifurcations meet, changing the overall rim shape into a 12-sided polygon (Pl. 1, figs 5, 6; Pl. 3, fig. 2; Aubry, 1993*b*, Pl. 16, figs 4–6).

The proximal side of *C. coalitus* features a stellate ray pattern whose orientation mirrors that of the same features on the distal side (Pl. 1, figs 5–6; Pl. 2, figs 16, 18) .

Catinaster coalitus coalitus Martini & Bramlette, 1963
(Pl. 1, figs 1–7; Pl. 2, figs 12–18)

Remarks. This subspecies is the type of the species *C. coalitus*. It is characterized by confinement of the rays within the rim. There may be gaps betwen the bifurcation tips, or they may meet neatly, or protrude to form pseudo–rays.

Catinaster coalitus extensus **n. subsp.**
(Pl. 1, figs 8–9; Pl. 2, figs 19–20; Pl. 3, figs 1–6)

Derivation of name. Latin, *extensus*, extend, referring to the rays that extend out of the basket.
Holotype. Pl. 1, fig. 8; SIO-NLC #019-001.
Holotype locality. Ocean Drilling Program Hole 782A on the eastern margin of the Izu-Bonin forearc basin, western Pacific Ocean (30° 51.66'N, 141° 18.85'E); ODP Sample 782A-26X-CC
Isotype. Pl. 2, fig. 19; SIO-NLC #018-002.
Isotype locality. Ocean Drilling Program Hole 710A in the central Madingley Rise, western equatorial Indian Ocean (04° 18.7'S, 60° 58.8'E); ODP Sample 710A-9H-5, 110–111 cm.
Diagnosis. *Catinaster coalitus extensus* has six rays which meet the middle of the segments of the hexagonal rim and extend out of it. The rays taper towards the tips and do not curve.
Size. 6–7 μm.
Remarks. *C. coalitus extensus* is similar to specimens of *C. coalitus coalitus* with hexagonal baskets except that in the latter, the arms do not extend out of the basket. It closely resembles *C. calyculus rectus* but differs from it in that the rays in *C. coalitus extensus* meet the middle of the segments rather the corners of the basket when seen in the light microscope. Also, the rays do not curve as in *C. calyculus calyculus*.
Occurrence. This nannofossil is found in well-preserved sites from mid to low latitudes. Abundance of this species is quite low. It usually occurs in nannofossil zones CN6 and CN7 and mostly correlates with the middle to upper part of magnetic chron C5n.2n but can extend to subchrons C5r.1 and C4Ar.2n in some sites. Its stratigraphic range is limited within the range of *C. coalitus coalitus*.

Catinaster calyculus Martini & Bramlette, 1963

1963 *Catinaster calyculus* Martini & Bramlette: 850, pl. 103, figs 1–6
1967 *Catinaster calyculus* Martini & Bramlette; Bramlette & Wilcoxon: 108, pl. 8, fig. 13
1971 *Catinaster calyculus* Martini & Bramlette; Martini: 784–785, pl. 4, fig. 5
1974 *Catinaster calyculus* Martini & Bramlette; Müller: 614–615, pl. 10, figs 9–12
1981 *Catinaster calyculus* Martini & Bramlette; Martini: 563, pl. 3, figs 6–9
1981 *Catinaster calyculus* Martini & Bramlette; Martini: 565, pl. 5, figs 3–6
1990 *Catinaster calyculus* Martini & Bramlette; Rio *et al.*: 227, pl. 6, fig. 13
1992 *Catinaster calyculus* Martini & Bramlette; Xu & Wise: 70, pl. 5, figs 5–6
1992 Non–*Catinaster calyculus* Martini & Bramlette; Jiang & Watkins: 617, pl. 3, figs 31–32
1993*b* *Catinaster calyculus* Martini & Bramlette; Aubry: 171, pl. 16, figs 7–10
1993*b* Non-*Catinaster calyculus* Martini & Bramlette; Aubry: 171, pl. 16, figs 11–14
1995 *Catinaster calyculus* Martini & Bramlette; Peleo-Alampay & Wei: 108, pl. 2, figs 5–9

Remarks. The shape of the rim in *C. calyculus* is modified from the simple hexagonal rim found in *C. coalitus*. Each of the extended rays of *C. calyculus* forms protruding corners with the simple hexagonal rim which has protracted proximally. This results in a modified hexagonal rim whose sharp corners are formed by the extended rays. When seen under the light microscope, the rays appear to meet the corners of the hexagonal basket rather than the middle of the segments as in *C. coalitus* (Peleo-Alampay & Wei, 1995). As in *C. coalitus* there are usually either well defined sutures or gaps between the rays on the proximal side which makes it easy to distinguish them (e.g. Pl. 1, figs 13–15). It is clear from such specimens that the ridges on the distal side are true rays, not inter–radial ridges (as in *C. mexicanus*). The parallelism of the distal and proximal structures can easily be observed in light microscopy by focusing through the specimens. It is a useful test that the specimen is a true catinaster.

Jiang & Watkins (1992) also showed micrographs of *C. calyculus* that are considered here as *C. coalitus coalitus*. Micrographs in Aubry (1993*b*; pl. 16, figs 11–14) identified as *C. calyculus* are considered as *C. coalitus coalitus* since the rays mostly hit the middle of the segments of the basket and its side view is more typical of *C. coalitus coalitus*.

Catinaster calyculus calyculus Martini & Bramlette, 1963
(Pl. 1, figs 16–20; Pl. 2, fig. 1; Pl. 3, figs 12–16)

Remarks. *C. calyculus calyculus* is the type of the species *C. calyculus*. It is distinguished from a new subspecies, *C. calyculus rectus* by its curved rays that bend counter–clockwise in distal view. This is the opposite sense of rotation to that shown by the co–eval *Discoaster* species *D. hamatus* and *D. calcaris,* which confirms that there is no direct evolutionary cause for the co–incidence of ray curvature in two separate lineages at this time.
Occurrence. This subspecies occurs later than *C. calyculus rectus*. The FO of *C. calyculus calyculus* is not completely consistent based on the sites studied, although it remains within magnetic chron C5n.2.

Catinaster calyculus rectus n. subsp.
(Pl. 1, figs 10–15; Pl. 3, figs 7–11)

Derivation of name. Latin, *rectus*, straight, referring to the straight arms of this *C. calyculus* subspecies.
Holotype. Pl. 1, fig. 11; SIO–NLC #018-003; ODP Sample 710A-9H-3, 30–31 cm.
Isotype. Pl. 3, fig. 7; SIO–NLC# 018–004; ODP Sample 710A-9H-4, 110–111 cm.
Type Locality. Both holotype and isotype are from Ocean Drilling Program Hole 710A in the central Madingley Rise, western equatorial Indian Ocean (04° 18.7'S, 60° 58.8'E).
Diagnosis. Catinaster with straight rays that may or may not extend out of the outer rim. Each ray extends to form a corner of the modified rim instead of meeting the rim at mid-segment as in *C. coalitus* (see *C. calyculus* description).
Occurrence. The FO of *C. calyculus rectus* is in the lower part of C5n.2n in some sites but has also been documented to occur later (mid–upper C5n.2n), suggesting diachroneity. Its LO is similar to that of *C. calyculus calyculus* but is slightly earlier in DSDP Sites 558, 563 and 588.

Catinaster mexicanus Bukry, 1971
(Pl. 2, figs 2–8; Pl. 3, figs 17–20)

1971 *Catinaster mexicanus* Bukry: 50, pl. 3, figs 7–9
1972 *Catinaster mexicanus* Bukry; Ellis, *et al.*: 37, pl. 10, fig. 1
1974 *Catinaster mexicanus* Bukry; Müller: 615, pl. 10, figs 6–7
1974 Non–*Catinaster mexicanus* Bukry; Müller: 633, pl. 19, fig. 2
1981 *Catinaster mexicanus* Bukry; Bukry: 466, pl. 1, figs 1–3
1992 Non–*Catinaster mexicanus* Bukry; Xu & Wise: 70, pl. 5, fig. 18
1993*a* *Catinaster mexicanus* Bukry; Aubry: 363, pl. 2, fig. 20

Remarks. *Catinaster mexicanus* has short bifurcate rays (Bukry, 1971) which do not extend beyond the rim of the basket. Adjacent bifurcations meet to form double-peaked protrusions of the rim. This results in an overall digitate appearance of the basket which makes it distinct from the other catinasters. Unlike the other catinasters, sutural ridges occur on the distal side of *C. mexicanus* between the rays and in opposite orientation to the radial ridges on the proximal side. This can easily be seen in light microscopy while focusing through the specimen, stellate structures are clearly visible on both sides of the specimen but with opposite orientation. In this respect *C.mexicanus* is similar to normal Neogene discoasters and differs from true catinasters. It differs from *C. calyculus calyculus* in the absence of long curved arms. The *C. mexicanus* micrographs in Müller (1974) and Xu & Wise (1992) do not show the characteristic digitate basket of this species.
Size. 4–6 MMMm.
Occurrence. *C. mexicanus* has been found in nannofossil zones CN7–CN9a (late Miocene), correlating to magnetic chrons C4A to C4n.

ACKNOWLEDGMENTS

We thank Wuchang Wei for encouraging us to do this study and for his valuable suggestions in improving the manuscipt. We are also grateful to two anonymous referees for their constructive and helpful reviews. This study was supported in part by grants from the U.S. Science Foundation and the Petroleum Research Fund (to W. Wei). Samples were supplied by the Ocean Drilling Program.

Manuscript received September 1996
Manuscript accepted January 1997

REFERENCES

Ali, J. R., Haston, R. B. & Stokking, L. B. 1992. Magnetostratigraphy of Sites 782, 783, 784, and 786, Izu–Bonin outer forearc, western Pacific. *Proceedings of the Ocean Drilling Program, Scientific Results*, **125:** 547–560.

Aubry, M. P. 1993a. Neogene allostratigraphy and depositional history of the De Soto Canyon area, northern Gulf of Mexico. *Micropaleontology*, **39:** 327–366.

Aubry, M. P. 1993b. Calcareous nannofossil stratigraphy of the Neogene formations of eastern Jamaica. *In* R. M. Wright & E. Robinson (Ed.), *Biostratigraphy of Jamaica*. 131–178. Geological Society of America Memoir 182.

Backman, J., Schneider, D. A., Rio, D. & Okada, H. 1990. Neogene low-latitude magnetostratigraphy from Site 710 and revised age estimates of Miocene nannofossil datum events. *Proceedings of the Ocean*

Drilling Program, Scientific Results, **115:** 271–276.

Barton, C. E. & Bloemendal, J. 1986. Paleomagnetism of sediments collected during Leg 90, southwest Pacific. *Initial Reports of the Deep Sea Drilling Project*, **90:** 1273–1316.

Berggren, W. A., Kent, D. V., Swisher, C. C. III & Aubry, M.-P. 1995. A revised Cenozoic geochronology and chronostratigraphy. *In* Berggren, W. A., Kent, D. V., Aubry, M.-P. & Hardenbol, J. (Eds), *Geochronology, Time Scales and Global Stratigraphic Correlation*, 129–212. SEPM Special Publication No. 54.

Bramlette, M. N. & Wilcoxon, J. A. 1967. Middle Tertiary nannoplankton of the Cipero Section, Trinidad, W.I. *Tulane Studies in Geology*, **5:** 93–131.

Bukry, D. 1971. Discoaster evolutionary trends. *Micropaleontology*, **17:** 43–52.

Bukry, D. 1973. Low-latitude coccolith biostratigraphic zonation. *Initial Reports of the Deep Sea Drilling Project*, **15:** 685–703.

Bukry, D. 1981. Pacific coast coccolith stratigraphy between Point Conception and Cabo Corrientes, Deep Sea Drilling Project Leg 63. *Initial Reports of the Deep Sea Drilling Project*, **63:** 445–471.

Bukry, D. & Bramlette, M. N. 1969. Coccolith age determinations: Leg 1, Deep Sea Drilling Project. *Initial Reports of the Deep Sea Drilling Project*, **1:** 369–387.

Cande, S. C. & Kent, D. V. 1992. A new geomagnetic polarity time scale for the Late Cretaceous and Cenozoic. *Journal of Geophysical Research*, **97:** 13 917–13 951.

Cande, S. C. & Kent, D. V. 1995. Revised calibration of the geomagnetic polarity timescale for the Late Cretaceous and Cenozoic. *Journal of Geophysical Research*, **100:** 6093–6095.

de Kaenel, E. & Villa, G. 1996. Oligocene–Miocene calcareous nannofossil biostratigraphy and paleoecology from the Iberia Abyssal Plain. *Proceedings of the Ocean Drilling Program, Scientific Results*, **149:** 79–145.

Ellis, C. H., Lohman, W. H. & Wray, J. L. 1972. Upper Cenozoic calcareous nannofossils from the Gulf of Mexico (Deep Sea Drilling Project Leg 1, Site 3). *Quarterly of the Colorado School of Mines*, **67:** 1–103.

Gartner, S. 1992. Miocene nannofossil chronology in the North Atlantic, DSDP Site 608. *Marine Micropaleontology*, **18:** 307–331.

Jiang, M. M. & Watkins, J. S. 1992. Floral pulses, foraminiferal peaks and inferred sequences in the Miocene of the northern Gulf of Mexico. *Marine and Petroleum Geology*, **9:** 608–622.

Kahn, M. J., Kent, D. V. & Miller, K. G. 1985. Magnetostratigraphy of Oligocene to Pleistocene sediments, Sites, 558 and 563. *Initial Reports of the Deep Sea Drilling Project*, **82:** 385–392.

Lohman, W. H. 1986. Calcareous nannoplankton biostratigraphy of the Southern Coral Sea, Tasman Sea, and Southwestern Pacific Ocean, Deep Sea Drilling Project Leg 90: Neogene and Quaternary. *Initial Reports of the Deep Sea Drilling Project*, **90:** 763–794.

Martini, E. 1971. Standard Tertiary and Quaternary calcareous nannofossil zonation. *In* Farinacci, A. (Ed.), *Proceedings of the II Planktonic Conference, Roma, 1970*, **2:** 739–786.

Martini, E. 1981. Oligocene to Recent calcareous nannoplankton from the Philippine Sea, Deep Sea Drilling Project Leg 59. *Initial Reports of the Deep Sea Drilling Project*, **59:** 547–565.

Martini, E. & Bramlette, M. N. 1963. Calcareous nannoplankton from the experimental Mohole drilling. *Journal of Paleontology*, **37:** 845–856.

Martini, E. & Worsley, T. R. 1971. Calcareous nannofossils from the western equatorial Pacific Leg 7. *Initial Reports of the Deep Sea Drilling Project, Part 2*, **7:** 1471–1507.

Mayer, L., Pisias, N., Janecek, T. *et al.* 1992. *Proceedings of the Ocean Drilling Program, Initial Reports*, **138**, 1–960.

Miller, K. G., Aubry, M. P., Khan, M. J., Melillo, A. J., Kent, D. V. & Berggren, W. A. 1985. Oligocene–Miocene biostratigraphy, magnetostratigraphy, and isotopic stratigraphy of the western North Atlantic. *Geology*, **13:** 257–261.

Miller, K. G., Wright, J. D., van Fossen, M. C. & Kent, D. V. 1994. Miocene stable isotopic stratigraphy and magnetostratigraphy of Buff Bay, Jamaica. *Geologic Society of America Bulletin*, **106**: 1605–1620.

Müller, C. 1974. Calcareous nannoplankton, Leg 25 (Western Indian Ocean). *Initial Reports of the Deep Sea Drilling Project*, **25:** 579–633

Okada, H. & Bukry, D. 1980. Supplementary modification and introduction of code numbers to the low-latitude coccolith biostratigraphic zonation (Bukry, 1973; 1975). *Marine Micropaleontology*, **5:** 321–325.

Parker, M. E., Clark, M. & Wise, S. W. Jr. 1985. Calcareous nannofossils of Deep Sea Drilling Project Sites 558 and 563, North Atlantic Ocean: Biostratigraphy and the distribution of Oligocene braarudosphaerids. *Initial Reports of the Deep Sea Drilling Project*, **82:** 559–589.

Peirce, J., Weissel, J. *et al.* 1989. *Proceedings of the Ocean Drilling Program, Initial Reports*, **121**, 1–990.

Peleo-Alampay, A. & Wei, W. 1995. Magnetobiochronology of several Miocene nannofossil datums at DSDP Site 563 revisited. *Revista Española de Micropaleontologia*, **27**: 97–110.

Perch-Nielsen, K. 1985. Cenozoic calcareous nannofossils. *In* Bolli, H. M. *et al. Plankton Stratigraphy* Vol. 1. 427–554. Cambridge University Press, Cambridge.

Percival, S. F. Jr 1984. Late Cretaceous to Pleistocene calcareous nannofossils from the South Atlantic, Deep Sea Drilling Project Leg 73. *Initial Reports of the Deep Sea Drilling Project*, **73:** 391–424.

Poore, R. Z., Tauxe, L., Percival, S. F. Jr., La Brecque, J. L. Wright, R., Petersen, N. P., Smith, C. C., Tucker, P. & Hsü, K. J. 1984. Late Cretaceous–Cenozoic magnetostratigraphic and biostratigraphic correlations for the South Atlantic Ocean, Deep Sea Drilling Project Leg 73. *Initial Reports of the Deep Sea Drilling Project*, **73:** 645–655.

Prins, B. 1971. Speculations on relations, evolution and stratigraphic distribution of discoasters. *In* A. Farinacci (Ed.), *Proceedings II Planktonic Conference, Roma, 1970*, **2:** 1017–1037.

Pujos, A. 1985. Cenozoic nannofossils, central equatorial Pacific, Deep Sea Drilling Project Leg 85. *Initial Reports of the Deep Sea Drilling Project*, **85:** 581–607.

Raffi, I. & Flores, J.-A. 1995. Pleistocene through Miocene calcareous nannofossils from eastern equatorial Pacific Ocean (Leg 138). *Proceedings of the Ocean Drilling Program, Scientific Reports*, **138:** 233–288.

Raffi, I., Rio, D., d'Atri, A. Fornaciari, E. & Rochetti, S. 1995. Quantitative distribution patterns and biomagnetostratigraphy of middle and late Miocene calcareous nannofossils from equatorial Indian and Pacific Oceans (Leg 115, 130 and 138). *Proceedings of the Ocean Drilling Program, Scientific Reports*, **138:** 479–502.

Rio, D., Fornaciari, E. & Raffi, I. 1990. Late Oligocene–Early Pleistocene calcareous nannofossils from western equatorial Indian Ocean (Leg 115). *Proceedings of the Ocean Drilling Program, Scientific Results*, **115:** 175–235.

Schneider, D. A. 1995. Paleomagnetism of some Leg 138 sediments: detailing Miocene magnetostratigraphy. *Proceedings of the Ocean Drilling Program, Scientific Results*, **138:** 59–72.

Stradner, H. & Papp, A. 1961. Tertiäre Discoasteriden aus Österreich und deren stratigraphische Bedeutung mit Hinweisen auf Mexico, Rumänien und Italien. *Jahrbuch der Geologischen Bundesanstalt (Wien)*, Special Vol. **7**, 1–159.

Takayama, T. 1993. Notes on Neogene calcareous nannofossil biostratigraphy of the Ontong Java Plateau and size variations of *Reticulofenestra* coccoliths. *Proceedings of the Ocean Drilling Program, Scientific Results*, **130:** 179–195.

Theodoridis, S. 1984. Calcareous nannofossil biozonation of the Miocene and revision of the helicoliths and discoasters. *Utrecht Micropaleontological Bulletins*, **32**, 271 pp.

Xu, Y. & Wise, S. W. 1992. Middle Eocene to Miocene calcareous nannofossils of Leg 125 from the western Pacific Ocean. *Proceedings of the Ocean Drilling Program*, **125:** 43–70.

Young, J. R., Flores, J.-A. & Wei, W. 1994. A Summary chart of Neogene nannofossil magnetobiostratigraphy. *Journal of Nannoplankton Research*, **16:** 21–27.